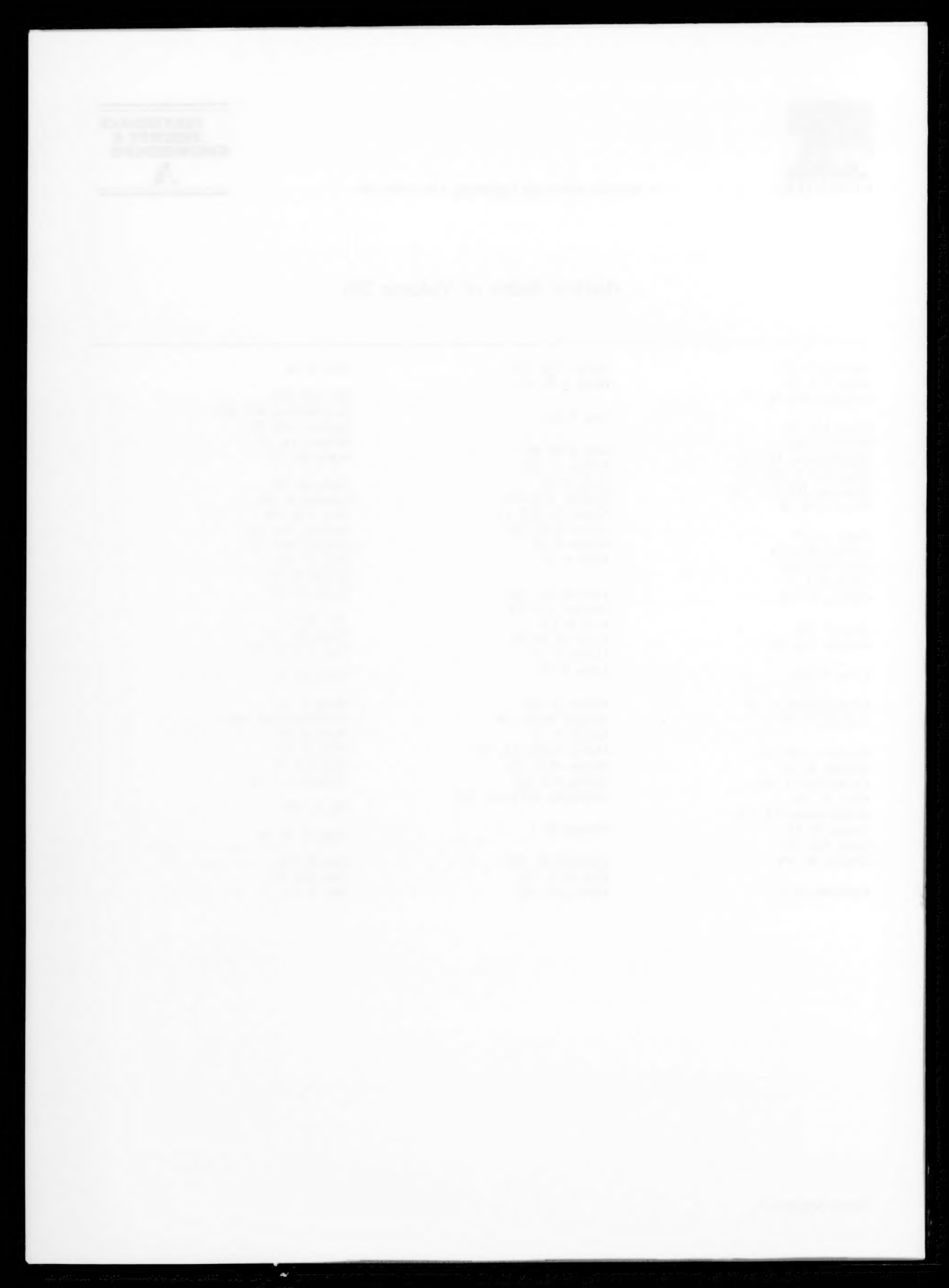




Author Index of Volume 201

-
- | | | |
|-------------------------|---------------------------|------------------------|
| Almqvist, N. 277 | Huang, C.M. 159 | Pink, E. 58 |
| Apgar, L.S. 169 | Huntz, A.M. 211 | Raj, S.V. 229 |
| Arsenault, R.J. 13 | Iung, T. L8 | Ravichandran, K.S. 269 |
| Baker, T.N. 257 | Klier, E.M. 88 | Redsten, A.M. 88 |
| Bartels, A. 182 | Koeppe, C. 182 | Romero, J.C. 13 |
| Bartholomeusz, M.F. 24 | Kong, S. 65 | Rubel, M. 277 |
| Batsanov, S.S. 150 | Krawitz, A.D. 134 | Saqib, M. 169 |
| Bhadeshia, H.K.D.H. 143 | Krause, Jr., R.F. 13 | Schretter, P. 182 |
| Brown, A.M. 88 | Kriven, W.M. 159 | Shin, D.H. 118 |
| Čadek, J. 127 | Kumar, S. 58 | Shipway, P.H. 143 |
| Cantrell, M.A. 24 | Kunz, L. 65 | Soliman, M.S. 111 |
| Chen, H.C. 150 | LaSalvia, J.C. 150 | Song, Y. 257 |
| Christ, H.-J. 1 | Lavernia, E.J. 118 | Stickler, R. 65 |
| Clemens, H. 182 | Li, G.B. L5 | Šustek, V. 127 |
| Dang, P. 194 | Li, J.C.M. 40, 50 | Tan, M. L1 |
| Dunand, D.C. 88 | LLorca, J. 77 | Tjong, S.C. L5 |
| Eylon, D. 169 | Lukas, P. 65 | Tsao, C.-Y.A. 261 |
| Fouilland-Paillé, L. 32 | Mackin, T. 159 | Violan, P. 32 |
| Franconi, E. 277 | Marquis, F.D.S. 150 | Wang, L. L5 |
| Gavrilkin, S.M. 150 | Martin, A. 77 | Weisbrook, C.M. 134 |
| Gerland, M. 32 | Medina Perilla, J.A. 103 | Weiss, B. 65 |
| Gil Sevillano, J. 103 | Meyers, M.A. 150 | Weiss, I. 169 |
| Glatz, W. 182 | Mishra, R.S. 205 | Wert, J.A. 24 |
| Gopalaratnam, V.S. 134 | Mukherjee, A.B.P.A.K. 205 | Williams, J.A. 242 |
| Grange, M. L8 | Öttinger, O. 1 | Xu, Y. 159 |
| Grant, N.J. 261 | Pahutová, M. 127 | Yang, F. 40, 50 |
| Grujicic, M. 194 | Park, K.-T. 118 | Zhu, D. 159 |
| Hoffmann, G. 1 | Parker, J.D. 242 | Zhu, S.M. L5 |
| | | Zhu, Y. L1 |



Subject Index of Volume 201

- AA6061 alloy**
 a calorimetric and metallographic study of precipitation process in AA6061 and its composites 257
- Al–Cu alloys**
 effect of Cu concentration on the high-temperature creep behavior of Al–Cu solid solution alloys 111
- Alloying**
 effects of in-situ alloying and microalloying on the microstructure and recrystallization behavior of spray-deposited SAE 1008 steel sheet 261
- Al₂O₃**
 thermal residual stresses in a Functionally Graded Material system 269
- 6061 Al/SiC composites**
 an evaluation of steady state creep mechanism in an Al–Mg/26 Al₂O₃f composite 205
- Aluminum**
 mechanical properties and microstructure of cast oxide-dispersion-strengthened aluminum 88
- Atomic force microscopy**
 surface characterization of SiC composites exposed to deuterium ions, using atomic force microscopy 277
- Austenitic materials**
 strains generated at austenitic:ferritic dissimilar welds during elastic pressure changes at high temperature 242
- Bainite**
 the effect of small stresses on the kinetics of the bainite transformation 143
- Calorimetry**
 a calorimetric and metallographic study of precipitation process in AA6061 and its composites 257
- Cavitation**
 microstructural changes during creep of an SiC/Al₂O₃ composite 13
- Ceramic reinforcement**
 a calorimetric and metallographic study of precipitation process in AA6061 and its composites 257
- Composite**
 interfacial properties of SiC monofilament reinforced β' -SiAlON composites 159
- Computer simulation**
 computer simulation of impression creep using the hyperbolic sine stress law 50
 computer simulation of martensitic transformation in Fe–Ni face-centered cubic alloys 194
- Copper**
 history effects in metals during constant and variable amplitude testing I: Wavy dislocation glide behaviour 1
- Creep**
 an evaluation of the properties of Cr₃Si alloyed with Mo 229
- microstructural changes during creep of an SiC/Al₂O₃ composite 13
- the enhanced work hardening rates of the constituent TiAl and Ti₃Al phases in a lamellar microstructure 24
- Creep behaviour**
 effect of Cu concentration on the high-temperature creep behavior of Al–Cu solid solution alloys 111
- Crystal defects**
 computer simulation of martensitic transformation in Fe–Ni face-centered cubic alloys 194
- Cr₃Si alloy**
 an evaluation of the properties of Cr₃Si alloyed with Mo 229
- Cyclic behaviour**
 cyclic behaviour of a 316L stainless steel hardened by an explosive treatment 32
- Cyclic deformation**
 history effects in metals during constant and variable amplitude testing I: Wavy dislocation glide behaviour 1
- Cyclic loading superposition**
 effect of cyclic loading superposition in the primary creep stage on the strain and fracture behaviour of 16Cr–10W–4Mo–TiAl nickel-base alloy 127
- Cyclic stress-strain response**
 cyclic stress-strain response and strain localization of polycrystalline Cu tested under stress-control and different start-up procedures 65
- Deuterium**
 surface characterization of SiC composites exposed to deuterium ions, using atomic force microscopy 277
- Dislocation**
 history effects in metals during constant and variable amplitude testing I: Wavy dislocation glide behaviour 1
- Dispersion strengthening**
 mechanical properties and microstructure of cast oxide-dispersion-strengthened aluminum 88
- Diffraction peak broadening**
 use of finite element modeling to interpret diffraction peak broadening from elastic strain distributions 134
- Elastic strain**
 strains generated at austenitic:ferritic dissimilar welds during elastic pressure changes at high temperature 242
- use of finite element modeling to interpret diffraction peak broadening from elastic strain distributions 134
- Explosive treatment**
 cyclic behaviour of a 316L stainless steel hardened by an explosive treatment 32
- Failure mechanisms**
 mechanical behaviour and failure mechanisms of a binary Mg–6%Zn alloy reinforced with SiC particulates 77

- Fatigue**
 history effects in metals during constant and variable amplitude testing I: Wavy dislocation glide behaviour 1
- Ferritic materials**
 strains generated at austenitic:ferritic dissimilar welds during elastic pressure changes at high temperature 242
- Fe–Ni alloys**
 computer simulation of martensitic transformation in Fe–Ni face-centered cubic alloys 194
- Fibre reinforced composites**
 a calorimetric and metallographic study of precipitation process in AA6061 and its composites 257
- Finite element method**
 mechanical behaviour of two-phase materials investigated by the finite element method: necessity of three-dimensional modeling L8
- Finite element modeling**
 use of finite element modeling to interpret diffraction peak broadening from elastic strain distributions 134
- Fracture**
 effect of cyclic loading superposition in the primary creep stage on the strain and fracture behaviour of 16Cr–10W–4Mo–TiAl nickel-base alloy 127
- Functionally Graded Material system**
 thermal residual stresses in a Functionally Graded Material system 269
- Growth stresses**
 stresses in NiO , Cr_2O_3 and Al_2O_3 oxide scales 211
- High temperature deformation**
 high-temperature deformation in a superplastic 7475 Al alloy with a relatively large grain size 118
- History effects**
 history effects in metals during constant and variable amplitude testing I: Wavy dislocation glide behaviour 1
- Hyperbolic sine stress law**
 computer simulation of impression creep using the hyperbolic sine stress law 50
- Impression creep**
 computer simulation of impression creep using the hyperbolic sine stress law 50
 impression test of 63Sn–37Pb eutectic alloy 40
- Incoloy 800H**
 laser surface alloying of Incoloy 800H with silicon carbide: microstructural aspects L5
- Interface**
 interfacial properties of SiC monofilament reinforced β' -SiAlON composites 159
- Joints**
 strains generated at austenitic:ferritic dissimilar welds during elastic pressure changes at high temperature 242
- Kinetics**
 the effect of small stresses on the kinetics of the bainite transformation 143
- Lamellar microstructure**
 the enhanced work hardening rates of the constituent TiAl and Ti_3Al phases in a lamellar microstructure 24
- Laser surface alloying**
 laser surface alloying of Incoloy 800H with silicon carbide: microstructural aspects L5
- Low-carbon steel**
 patterns of serrated flow in a low-carbon steel 58
- Martensitic transformation**
 computer simulation of martensitic transformation in Fe–Ni face-centered cubic alloys 194
- Mechanical behaviour**
 mechanical behaviour and failure mechanisms of a binary Mg–6%Zn alloy reinforced with SiC particulates 77
 mechanical behaviour of two-phase materials investigated by the finite element method: necessity of three-dimensional modeling L8
- Mechanical properties**
 mechanical properties and microstructure of cast oxide-dispersion-strengthened aluminum 88
- Mechanical testing**
 optimizing the properties of TiAl sheet material for application in heat protection shields or propulsion systems 182
- Mg–6%Zn alloy**
 mechanical behaviour and failure mechanisms of a binary Mg–6%Zn alloy reinforced with SiC particulates 77
- Microalloying**
 effects of in-situ alloying and microalloying on the microstructure and recrystallization behavior of spray-deposited SAE 1008 steel sheet 261
- Microstructure**
 laser surface alloying of Incoloy 800H with silicon carbide: microstructural aspects L5
 mechanical properties and microstructure of cast oxide-dispersion-strengthened aluminum 88
 microstructural changes during creep of an $\text{SiC}/\text{Al}_2\text{O}_3$ composite 13
 microstructure and phase morphology during thermochemical processing of α_2 -based titanium aluminide castings 169
 optimizing the properties of TiAl sheet material for application in heat protection shields or propulsion systems 182
- Molybdenum**
 thermal stability of nanostructured materials Ti, Ti_xN , Mo and Mo_2N L1
- Mo–Si**
 effect of shock pressure and plastic strain on chemical reactions in Nb–Si and Mo–Si systems 150
- Nanostructure**
 thermal stability of nanostructured materials Ti, Ti_xN , Mo and Mo_2N L1
- Nb–Si**
 effect of shock pressure and plastic strain on chemical reactions in Nb–Si and Mo–Si systems 150
- Nickel**
 thermal residual stresses in a Functionally Graded Material system 269
- Nickel-base alloy**
 effect of cyclic loading superposition in the primary creep stage on the strain and fracture behaviour of 16Cr–10W–4Mo–TiAl nickel-base alloy 127
- Oxidation properties**
 an evaluation of the properties of Cr_3Si alloyed with Mo 229
- Oxide scales**
 stresses in NiO , Cr_2O_3 and Al_2O_3 oxide scales 211
- Phase morphology**
 microstructure and phase morphology during thermochemical processing of α_2 -based titanium aluminide castings 169
- Plastic strain**
 effect of shock pressure and plastic strain on chemical reactions in Nb–Si and Mo–Si systems 150
- Polycrystalline Cu**
 cyclic stress-strain response and strain localization of polycrystalline Cu tested under stress-control and different start-up procedures 65

- Primary creep**
 effect of cyclic loading superposition in the primary creep stage on the strain and fracture behaviour of 16Cr-10W-4Mo-TiAl nickel-base alloy 127
- Recrystallization behaviour**
 effects of in-situ alloying and microalloying on the microstructure and recrystallization behavior of spray-deposited SAE 1008 steel sheet 261
- Serrations**
 patterns of serrated flow in a low-carbon steel 58
- Shear stress**
 two-dimensional sections of the yield locus of a Ti-6%Al-4%V alloy with a strong transverse-type crystallographic α -texture 103
- Shock pressure**
 effect of shock pressure and plastic strain on chemical reactions in Nb-Si and Mo-Si systems 150
- β' -SiAlON**
 interfacial properties of SiC monofilament reinforced β' -SiAlON composites 159
 SiC/Al₂O₃ composite microstructural changes during creep of an SiC/Al₂O₃ composite 13
 microstructural changes during creep of an SiC/Al₂O₃ composite 13
- SiC fibre reinforcement**
 interfacial properties of SiC monofilament reinforced β' -SiAlON composites 159
- SiC particles**
 laser surface alloying of Incoloy 800H with silicon carbide: microstructural aspects L5
- SiC particulates**
 mechanical behaviour and failure mechanisms of a binary Mg-6%Zn alloy reinforced with SiC particulates 77
- Silicon carbide**
 surface characterization of SiC composites exposed to deuterium ions, using atomic force microscopy 277
- Sn-Pb eutectic alloy**
 impression test of 63Sn-37Pb eutectic alloy 40
- Spray deposited 1008 steel**
 effects of in-situ alloying and microalloying on the microstructure and recrystallization behavior of spray-deposited SAE 1008 steel sheet 261
- Stainless steel**
 cyclic behaviour of a 316L stainless steel hardened by an explosive treatment 32
- Steady state creep**
 an evaluation of steady state creep mechanism in an Al-Mg/26 Al₂O₃f composite 205
- Steels**
 the effect of small stresses on the kinetics of the bainite transformation 143
- Strain**
 effect of cyclic loading superposition in the primary creep stage on the strain and fracture behaviour of 16Cr-10W-4Mo-TiAl nickel-base alloy 127
- Strain rates**
 patterns of serrated flow in a low-carbon steel 58
- Stress**
 the effect of small stresses on the kinetics of the bainite transformation 143
- Stress control**
 cyclic stress-strain response and strain localization of polycrystalline Cu tested under stress-control and different start-up procedures 65
- Stress relaxation**
 impression test of 63Sn-37Pb eutectic alloy 40
 stresses in NiO, Cr₂O₃ and Al₂O₃ oxide scales 211
- Superplastic 7475 Al alloy**
 high-temperature deformation in a superplastic 7475 Al alloy with a relatively large grain size 118
- Surface roughness**
 surface characterization of SiC composites exposed to deuterium ions, using atomic force microscopy 277
- Temperature dependence**
 an evaluation of steady state creep mechanism in an Al-Mg/26 Al₂O₃f composite 205
- Tensile tests**
 high-temperature deformation in a superplastic 7475 Al alloy with a relatively large grain size 118
- Texture**
 two-dimensional sections of the yield locus of a Ti-6%Al-4%V alloy with a strong transverse-type crystallographic α -texture 103
- Thermal residual stresses**
 thermal residual stresses in a Functionally Graded Material system 269
- Thermal stability**
 thermal stability of nanostructured materials Ti, Ti_xN, Mo and Mo₂N L1
- Thermal stresses**
 stresses in NiO, Cr₂O₃ and Al₂O₃ oxide scales 211
- Thermochemical processing**
 microstructure and phase morphology during thermochemical processing of α_2 -based titanium aluminide castings 169
- Three-dimensional modeling**
 mechanical behaviour of two-phase materials investigated by the finite element method: necessity of three-dimensional modeling L8
- TiAl**
 the enhanced work hardening rates of the constituent TiAl and Ti₃Al phases in a lamellar microstructure 24
- Ti₃Al**
 the enhanced work hardening rates of the constituent TiAl and Ti₃Al phases in a lamellar microstructure 24
- Ti-6%Al-4%V alloy**
 two-dimensional sections of the yield locus of a Ti-6%Al-4%V alloy with a strong transverse-type crystallographic α -texture 103
- TiAl sheets**
 optimizing the properties of TiAl sheet material for application in heat protection shields or propulsion systems 182
- Titanium**
 thermal stability of nanostructured materials Ti, Ti_xN, Mo and Mo₂N L1
- Titanium aluminide castings**
 microstructure and phase morphology during thermochemical processing of α_2 -based titanium aluminide castings 169
- Transmission electron microscopy**
 laser surface alloying of Incoloy 800H with silicon carbide: microstructural aspects L5
- Two-phase materials**
 mechanical behaviour of two-phase materials investigated by the finite element method: necessity of three-dimensional modeling L8
- WC-Ni composites**
 use of finite element modeling to interpret diffraction peak broadening from elastic strain distributions 134
- Work hardening**
 the enhanced work hardening rates of the constituent TiAl and Ti₃Al phases in a lamellar microstructure 24

